Epitaxial integration of (0001) Bi Fe O 3 with (0001) GaN

W. Tian, V. Vaithyanathan, D. G. Schlom, Q. Zhan, S. Y. Yang, Y. H. Chu, and R. Ramesh

Citation: Applied Physics Letters **90**, 172908 (2007); doi: 10.1063/1.2730580
View online: http://dx.doi.org/10.1063/1.2730580
View Table of Contents: http://scitation.aip.org/content/aip/journal/apl/90/17?ver=pdfcov
Published by the AIP Publishing

Epitaxial integration of (0001) $BiFeO_3$ with (0001) GaN

W. Tian, V. Vaithyanathan,[a] and D. G. Schlom[b]
Department of Materials Science and Engineering, Pennsylvania State University, Pennsylvania 16802-5005

Q. Zhan, S. Y. Yang, Y. H. Chu, and R. Ramesh
Department of Materials Science and Engineering, University of California, Berkeley, California 94720 and Department of Physics, University of California, Berkeley, California 94720

(Received 2 October 2006; accepted 23 March 2007; published online 25 April 2007)

Epitaxial growth of (0001)-oriented $BiFeO_3$ thin films on the (0001) surface of GaN has been realized using intervening epitaxial (111) $SrTiO_3$/(100) TiO_2 buffer layers. The epitaxial $BiFeO_3$ thin films have two in-plane orientations: $[11\bar{2}0]BiFeO_3 \| [11\bar{2}0]GaN$ plus a twin variant related by a 180° in-plane rotation. $BiFeO_3$ shows an out-of-plane remanent polarization of ~90 $\mu C/cm^2$, which is comparable to the remanent polarization of $BiFeO_3$ prepared on (111) $SrTiO_3$ single crystal substrates. The orientation of $BiFeO_3$ realized on GaN provides the maximal out-of-plane polarization of $BiFeO_3$, which is equivalent to a surface charge of 5×10^{14} electrons/cm^2.
 [DOI: 10.1063/1.2730580]

The integration of multifunctional oxides including ferroelectrics, ferromagnets, and multiferroics with semiconductors is being pursued to enable a variety of devices with enhanced performance.[1–4] Integrating ferroelectric oxides with (0001)-oriented nitrides is of particular interest due to the polar nature of the (0001) surfaces of nitrides and the switchable polar nature of ferroelectrics. Such integration could lead to junctions with tailorable *I-V* characteristics and channels with very high conductivities.[2] Due to the anisotropic properties of ferroelectric oxides, e.g., the spontaneous polarization being aligned with specific crystallographic orientations, it is important to orient them optimally for particular applications. Epitaxy is a viable means to achieve such orientation control. Additionally, epitaxial films are desirable because randomly oriented polycrystalline films possess grain-to-grain variation in their out-of-plane remanent polarization (P_r) that put constraints on device scaling as the feature size approaches the grain size.[5]

The ferroelectrics that have been epitaxially integrated with (0001) GaN include $Ba_{0.5}Sr_{0.5}TiO_3$,[6] La-substituted $Bi_4Ti_3O_{12}$,[7] and $YMnO_3$.[8,9] The out-of-plane P_r reported in these studies range from 3 to 22 $\mu C/cm^2$.

In this work, we show that a much larger out-of-plane P_r can be realized by optimally orienting epitaxial $BiFeO_3$ thin films with their polarization axes normal to the (0001) surface of GaN. Films of the multiferroic $BiFeO_3$ have P_r values among the highest of any known ferroelectric. For instance, (0001)-oriented epitaxial $BiFeO_3$ thin films prepared on (111) $SrTiO_3$ substrates show P_r greater than 100 $\mu C/cm^2$.[10–12] The spontaneous polarization of bulk $BiFeO_3$ lies along the [0001] axis. Thus, it is desirable to align $BiFeO_3$ with its [0001] axis perpendicular to the plane of the substrate for many device applications.[2–4] We have achieved this desired orientation of $BiFeO_3$ on GaN using intermediate epitaxial $SrTiO_3/TiO_2$ buffer layers.

In bulk, $BiFeO_3$ has a rhombohedral structure with space group $R3c$ with $a=5.5787$ Å, $c=13.8688$ Å, and $\gamma=120°$ when indexed with hexagonal indices.[13] It can also be considered as a pseudocubic perovskite with $a \approx 3.96$ Å. We use hexagonal indexing for $BiFeO_3$ in this letter.

Unlike $YMnO_3$,[8,9] direct deposition of $BiFeO_3$ on (0001) GaN results in approximately randomly oriented polycrystalline thin films.[14] To epitaxially orient $BiFeO_3$ with its [0001] axis normal to the (0001) surface of GaN, appropriate buffer layers are needed. (111)-oriented $SrTiO_3$ substrates are known to work well in this regard.[10–12] Our previous studies have demonstrated the growth of (100)-oriented epitaxial rutile TiO_2 on (0001) GaN.[15] In the present work we grow (111) $SrTiO_3$ epitaxially on (100) TiO_2 on GaN, enabling the epitaxial integration of (0001) $BiFeO_3$ with (0001) GaN.

In this work, a heterostructure composed of an epitaxially (0001)-oriented $BiFeO_3$ on an underlying epitaxially (111)-oriented $SrRuO_3$ bottom electrode on the (111) $SrTiO_3$/(100) TiO_2 buffer layers grown on the (0001) surface of GaN was prepared and characterized structurally and electrically. The epitaxial (100) TiO_2 layer and overlying (111)-oriented epitaxial $SrTiO_3$ were grown on commercially available (0001) GaN-on-sapphire substrates[16] by reactive molecular-beam epitaxy (MBE). The MBE setup is described in detail elsewhere.[17] Following the growth of the intermediate buffer layers, $BiFeO_3$ thin films were grown by metal-organic chemical vapor deposition equipped with a liquid-delivery system.[18] Triphenylbismuth [$Bi(Ph)_3$] and tris(2,2,6,6-tetramethyl-3,5-heptanedionate)iron [$Fe(thd)_3$] dissolved in tetrahydrofuran were used as the liquid metal-organic precursor materials. The supply rates for the bismuth and iron sources were 7.8×10^{-6} and 1.22×10^{-6} mol/min, respectively, and the substrate was held 620 °C during deposition. The heterostructures were structurally characterized *in situ* by reflection high-energy electron diffraction (RHEED) during MBE and *ex situ* by four-circle x-ray diffraction (XRD) and transmission electron microscopy (TEM). High-resolution TEM (HRTEM) performed in a Philips CM200 was used to characterize the atomic structure of the (111) $SrTiO_3$/(100) TiO_2 interface. The ferroelectric properties of the $BiFeO_3$ thin films were measured using a Radiant Technologies 6000 ferroelectric test system.

Prior to growth of the oxide layers, the GaN-on-sapphire substrates were etched using a $HCl:H_2O=1:1$ solution for 2 min. An epitaxial rutile TiO_2 layer was then grown at a

[a]Present address: Seagate Technology, Pittsburgh, PA 15222.
[b]Electronic mail: schlom@ems.psu.edu

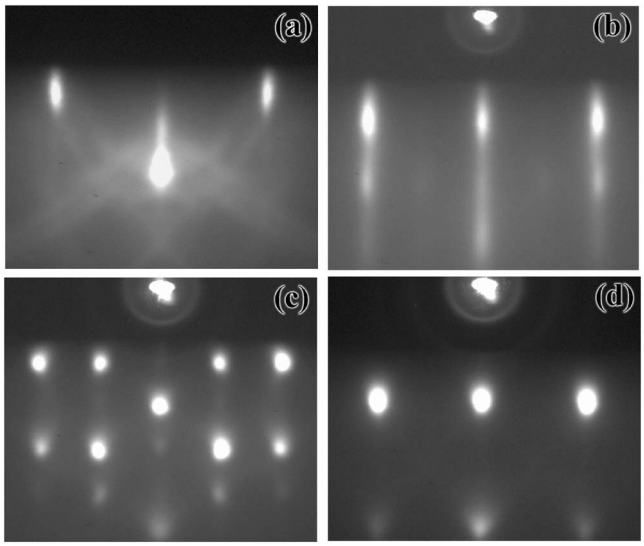

FIG. 1. (Color online) RHEED patterns during the growth of a $SrTiO_3/TiO_2/GaN$ heterostructure. (a) Bare GaN substrate at T_{sub} ~600 °C and (b) after the growth of a 30 nm thick rutile TiO_2 layer viewed along the $[11\bar{2}0]$ azimuth of GaN. [(c) and (d)] RHEED patterns of the 20 nm thick $SrTiO_3$ layer completing the heterostructure viewed along the $[11\bar{2}0]$ and the $[10\bar{1}0]$ azimuths of GaN, respectively.

substrate temperature of ~600 °C in an oxygen background pressure of 1×10^{-6} Torr. For growth of the epitaxial $SrTiO_3$ layer, the strontium and titanium molecular beams were shuttered to supply monolayer doses of strontium and titanium to the substrate in a sequential manner consistent with the desired (111) $SrTiO_3$ film growth by alternating monolayers of SrO_3 and Ti at a substrate temperature of 650 °C and an oxygen background pressure of 1×10^{-6} Torr.

Figure 1 shows the RHEED patterns recorded *in situ* during the growth of the TiO_2 and $SrTiO_3$ epitaxial layers. The $SrTiO_3$ diffraction pattern Fig. 1(c) and 1(d) are spotty, signifying three-dimensional growth.

Four-circle XRD was used to examine the epitaxial orientation relationship of the epitaxial $SrTiO_3$ and TiO_2 buffer layers. The θ-2θ and ϕ scans (not shown) indicate that this relationship is $(111)[1\bar{1}0]SrTiO_3\|(100)[001]TiO_2\|(0001)\langle11\bar{2}0\rangle GaN$. The epitaxial (100) TiO_2 layer has three twin variants related by 120° in-plane rotations (the three equivalent $\langle11\bar{2}0\rangle$ directions), as reported previously.[15] In contrast, the overlying epitaxial (111) $SrTiO_3$ has two twin variants related by a 180° in-plane rotation. As we shall show, the overlying epitaxial $BiFeO_3$ film inherits its orientation from the underlying $SrTiO_3$ buffer layer.

Figure 2(a) shows the θ-2θ XRD scan of a $BiFeO_3/SrRuO_3/SrTiO_3/TiO_2/GaN$ heterostructure. The 000ℓ Bragg reflections of $BiFeO_3$ are labeled. The scan shows that the $BiFeO_3$ is aligned with its [0001] axis normal to the (0001) surface of GaN. The presence of a small amount of $(10\bar{1}1)$-oriented $BiFeO_3$ cannot completely be ruled out, however, due to the overlap of the $BiFeO_3$ $20\bar{2}2$ and $40\bar{4}4$ peaks with the 111 and 222 peaks of $SrTiO_3$ and $SrRuO_3$.[19,20] The scan also shows that the $SrRuO_3$ bottom electrode is (111)-oriented out of plane. The full width at half maximum (FWHM) of the rocking curve of the 0006 reflection of $BiFeO_3$ is 0.37°, indicating comparable structural quality to $BiFeO_3$ grown on $SrTiO_3$ substrates.[12] Figure 2(b)

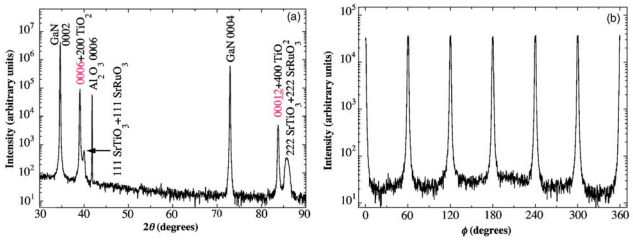

FIG. 2. (Color online) (a) θ-2θ x-ray diffraction scan of a 300 nm $BiFeO_3$/70 nm $SrRuO_3$/20 nm $SrTiO_3$/30 nm TiO_2/GaN heterostructure, indicating that the $BiFeO_3$ films are (0001) oriented. (b) XRD ϕ scan of the $BiFeO_3$ $10\bar{1}4$ reflection showing the $BiFeO_3$ film to be epitaxial with an in-plane orientation relationship of $[11\bar{2}0]BiFeO_3\|[11\bar{2}0]GaN$ plus a 180° in-plane rotational twin variant. ϕ=0° is aligned to be parallel to the $[10\bar{1}0]$ in-plane projection of the (0001) GaN substrate.

shows a ϕ scan of the $10\bar{1}4$ reflection of $BiFeO_3$. This reflection is selected to definitively determine the in-plane orientation of $BiFeO_3$. The FWHM of the $10\bar{1}4$ peak in ϕ is about 1.0°. Although $BiFeO_3$ has a threefold symmetry about the [0001] axis, the presence of $10\bar{1}4$ reflections every 60° in ϕ indicates that the $BiFeO_3$ film is twinned in the growth plane by a 180° in-plane rotation, just like the $SrTiO_3$ it grew on. The nearly equal intensities of all of the peaks indicate that the two twin variants have comparable populations. Together these scans reveal the epitaxial growth of $BiFeO_3$ with an orientation relationship with respect to GaN of (0001) $\times[11\bar{2}0]BiFeO_3\|(0001)[11\bar{2}0]$ GaN plus a twin variant related by a 180° in-plane rotation.

In contrast to the in-plane alignment of epitaxial $YMnO_3$ thin films grown on GaN,[8,9] a 30° in-plane rotation is not observed between the hexagonal unit cells of $BiFeO_3$ and GaN: the hexagonal bases of the $BiFeO_3$ and GaN are aligned with each other. As the $BiFeO_3$ inherits its orientation from the underlying $SrTiO_3$ layer, a key to understanding this orientation relationship is the alignment between the $SrTiO_3$ and TiO_2 films in the buffer layer. The epitaxial orientation relationship between the epitaxial (100) rutile TiO_2 thin film and the GaN substrate has been previously discussed.[15] We, therefore, focus on the orientation relationship between the epitaxial $SrTiO_3$ and rutile TiO_2 films.

TEM and HRTEM were used to examine the same $SrTiO_3/TiO_2$ buffer layers characterized in Fig. 1. Figure 3(a) shows a low magnification cross-sectional TEM image of the entire $SrTiO_3/TiO_2/GaN$ heterostructure. One can see that the interfaces between different layers are clean and well defined. The surface of the $SrTiO_3$ layer is rough, consistent with the spotty RHEED patterns shown in Figs. 1(c) and 1(d). Figure 3(b) shows a selected-area electron diffraction (SAED) pattern of the heterostructure with the incident electron beam along the $[11\bar{2}0]$ zone axis of GaN. This pattern is identified as a superimposition of two [110] zone axis SAED patterns of $SrTiO_3$ (indicated by the black solid and dashed rectangles, respectively), one [001] zone axis SAED pattern of rutile TiO_2 (indicated by a white solid rectangle), and one $[11\bar{2}0]$ zone axis SAED pattern of GaN (indicated by a white dashed rectangle). Figure 3(c) shows a cross-sectional HRTEM image of the (111) $SrTiO_3$/(100) TiO_2 interface. The interface is sharp and free of any reaction phases. The occurrence of in-plane twinning of the $SrTiO_3$ and TiO_2 layers has also been confirmed by

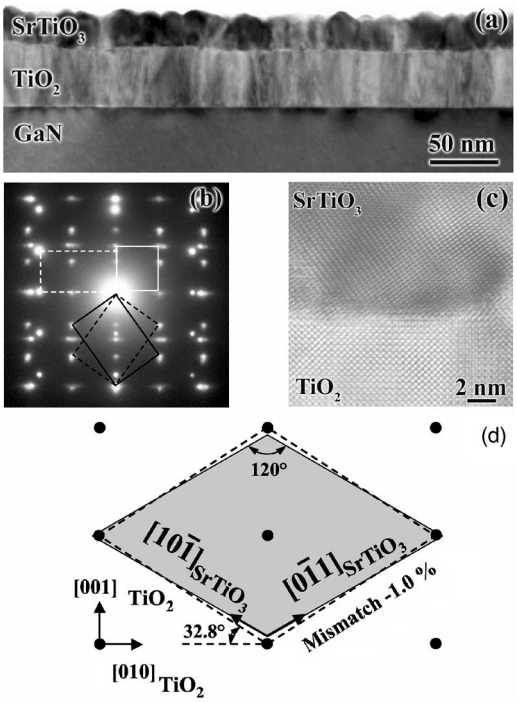

FIG. 3. (Color online) (a) Low magnification cross-sectional TEM image of the $SrTiO_3/TiO_2/GaN$ heterostructure characterized in Fig. 1. (b) Selected-area electron diffraction (SAED) pattern of the heterostructure with the incident electron beam along the $[11\bar{2}0]$ zone axis of GaN. (c) HRTEM image of the $SrTiO_3/TiO_2$ interface. (d) Schematic showing the in-plane epitaxial orientation relationship between (111) $SrTiO_3$ and (100) TiO_2. The black dots represent the lattice points of the (100) surface of TiO_2. The solid diamond represents the (111) surface unit cell of $SrTiO_3$. The near-coincident site lattice surface cell is indicated by the dashed line.

plan-view TEM characterization (images not shown).

Figure 3(d) schematically shows the observed in-plane epitaxial alignment between the (111) $SrTiO_3$ and (100) TiO_2. Rutile TiO_2 has a tetragonal structure with lattice constants $a=b=4.5933$ Å and $c=2.9592$ Å.[21] $SrTiO_3$ is cubic with lattice constant $a=3.905$ Å.[20] As shown in Fig. 3(d), the near-coincident site lattice (NCSL) surface cell indicated by the dashed line is twice as large as the (100) surface unit cell of TiO_2. The $[0\bar{1}1]$ direction of $SrTiO_3$ [the solid diamond represents the (111) surface unit cell of $SrTiO_3$] lies nearly along the [011] direction of TiO_2 with a slight tilt of 2.8°. The corresponding lattice mismatch is −1.0%, defined as $(\sqrt{a_{TiO_2}^2+c_{TiO_2}^2}-\sqrt{2}a_{SrTiO_3})/\sqrt{2}a_{SrTiO_3}$. Note that the identical NCSL surface cell results when the $SrTiO_3$ undergoes an in-plane rotation of 180°. Our schematic of the favorable epitaxial alignment between (111) $SrTiO_3$ and (100) TiO_2 is consistent with the observed unrotated epitaxial orientation relationship between $BiFeO_3$ and GaN.

The electric-displacement–electric-field hysteresis measured at 20 kHz and room temperature of the same heterostructure characterized by XRD in Fig. 2 is shown in Fig. 4. For the capacitor structure, circular platinum pads with a diameter of 32 μm were deposited as top electrodes using a standard lift-off process. The P_r and the coercive field (E_C) were determined to be ~90 $\mu C/cm^2$ and 470 kV/cm, respectively. This polarization value is consistent with one-half of the switched polarization $\Delta P=[P^*$ (switched polarization) $-P^\wedge$ (nonswitched polarization)$]\approx 190$ $\mu C/cm^2$. The measured P_r is comparable to that of $BiFeO_3$ prepared on (111) $SrTiO_3$ substrates[10–12] and by far the largest switchable polarization reported for any material on GaN.

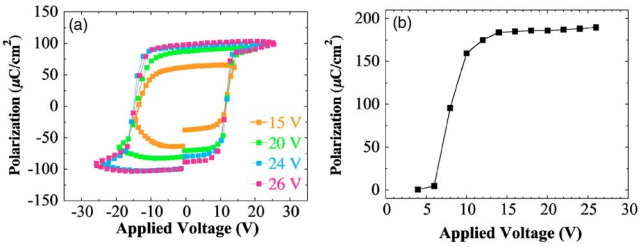

FIG. 4. (Color online) (a) Electric-displacement–electric-field hysteresis loops measured at 20 kHz at different voltage amplitudes and (b) switching polarization $[\Delta P=P^*$(switched polarization)$-P^\wedge$(nonswitched polarization)$]$ of the same heterostructure characterized by XRD in Fig. 2.

The authors gratefully acknowledge the financial support of the Office of Naval Research (ONR) under Grant Nos. N00014-03-1-0721, N00014-04-1-0426, and N00014-04-1-0426 monitored by Colin Wood. Partial support from a LBL LDRD is also gratefully acknowledged.

[1] W. A. Doolittle, G. Namkoong, A. G. Carver, and A. S. Brown, Solid-State Electron. **47**, 2143 (2003).
[2] M. Singh, Y.-R. Wu, and J. Singh, Solid-State Electron. **47**, 2155 (2003).
[3] Y.-R. Wu and J. Singh, Appl. Phys. Lett. **85**, 1223 (2004).
[4] Y.-R. Wu and J. Singh, IEEE Trans. Electron Devices **52**, 284 (2005).
[5] A. Gruverman, Appl. Phys. Lett. **75**, 1452 (1999).
[6] J.-Y. Hwang, J.-P. Kim, S.-Y. Jeong, S.-G. Yoon, and W.-J. Lee, Jpn. J. Appl. Phys., Part 2 **43**, L1425 (2004).
[7] C.-R. Cho, J.-Y. Hwang, J.-P. Kim, S.-Y. Jeong, and B. H. Park, Jpn. J. Appl. Phys., Part 1 **43**, 7625 (2004).
[8] A. Posadas, J.-B. Yau, C. H. Ahn, J. Han, S. Gariglio, K. Johnston, K. M. Rabe, and J. B. Neaton, Appl. Phys. Lett. **87**, 171915 (2005).
[9] Y. Chye, T. Liu, D. Li, K. Lee, D. Lederman, and T. H. Myers, Appl. Phys. Lett. **88**, 132903 (2006).
[10] J. Wang, J. B. Neaton, H. Zheng, V. Nagarajan, S. B. Ogale, B. Liu, D. Viehland, V. Vaithyanathan, D. G. Schlom, U. V. Waghmare, N. A. Spaldin, K. M. Rabe, M. Wuttig, and R. Ramesh, Science **299**, 1719 (2003).
[11] J. F. Li, J. L. Wang, M. Wuttig, R. Ramesh, N. G. Wang, B. Ruette, A. P. Pyatakov, A. K. Zvezdin, and D. Viehland, Appl. Phys. Lett. **84**, 5261 (2004).
[12] R. R. Das, D. M. Kim, S. H. Baek, C. B. Eom, F. Zavaliche, S. Y. Yang, R. Ramesh, Y. B. Chen, X. Q. Pan, X. Ke, M. S. Rzchowski, and S. K. Streiffer, Appl. Phys. Lett. **88**, 242904 (2006).
[13] F. Kubel and H. Schmid, Acta Crystallogr., Sect. B: Struct. Sci. **B46**, 698 (1990).
[14] Y. S. Yang, Q. Zhan, and R. Ramesh (unpublished).
[15] P. J. Hansen, V. Vaithyanathan, Y. Wu, T. Mates, S. Heikman, U. K. Mishra, R. A. York, D. G. Schlom, and J. S. Speck, J. Vac. Sci. Technol. B **23**, 499 (2005).
[16] 3.5 μm thick, non-intentionally doped, Ga face (0001) GaN films grown on (0001) Al_2O_3 substrates from Lumilog, Inc. (Vallauris, France).
[17] J. H. Haeni, C. D. Theis, and D. G. Schlom, J. Electroceram. **4**, 385 (2000).
[18] S. Y. Yang, F. Zavaliche, L. Mohaddes-Ardabili, V. Vaithyanathan, D. G. Schlom, Y. J. Lee, Y. H. Chu, M. P. Cruz, Q. Zhan, T. Zhao, and R. Ramesh, Appl. Phys. Lett. **87**, 102903 (2005).
[19] $SrTiO_3$ has a cubic perovskite structure with $a=3.905$ Å. $SrRuO_3$ has an orthorhombic structure but can be considered as a pseudocubic perovskite with $a\approx 3.925$ Å.
[20] *Landolt-Börnstein: Numerical Data and Functional Relationships in Science and Technology*, edited by K.-H. Hellwege and A. M. Hellwege, New Series, Group III (Springer, New York, 1981), Vol. 16, Pt. A, p. 59; (Springer, Berlin, 1977), Vol. 7, Pt. F, p. 734.
[21] *Landolt-Börnstein: Numerical Data and Functional Relationships in Science and Technology*, edited by Y. Shiozaki, E. Nakamura, and T. Mitsui, New Series, Group III (Springer, New York, 2001), Vol. 36, Pt. A2, p. 432.